Applied Catalysis B: Environmental 181 (2016) 644–650

Contents lists available at ScienceDirect

Applied Catalysis B: Environmental

journal homepage: www.elsevier.com/locate/apcatb

The impact of CO and C_3H_6 pulses on PtO_x reduction and NO oxidation in a diesel oxidation catalyst

Adéla Arvajová [a], Petr Kočí [a,*], Volker Schmeißer [b], Michel Weibel [b]

[a] University of Chemistry and Technology, Prague, Department of Chemical Engineering, Technická 5, 166 28 Prague, Czech Republic
[b] Daimler AG, 70546 Stuttgart, Germany

ARTICLE INFO

Article history:
Received 16 June 2015
Received in revised form 30 July 2015
Accepted 4 August 2015
Available online 11 August 2015

Keywords:
Diesel oxidation catalyst
Platinum oxide
Catalyst deactivation
Catalyst reactivation
Inverse hysteresis

ABSTRACT

A reversible deactivation of a diesel oxidation catalyst (DOC) due to the platinum oxide (PtO_x) formation is observed under lean conditions. Among others, the gradual build-up of PtO_x leads to a decreasing activity for NO oxidation. It is known that PtO_x formation is caused by O_2 and NO_2 present in the gas mixture and that platinum oxide can be reduced by NO at lower temperatures or thermally decomposed at high temperatures. In this paper we present experimental and modeling results showing that PtO_x can be reduced also by CO and C_3H_6 pulses.

First, temperature ramps from 120 to 420 °C and back to 120 °C were performed with a constant inlet gas composition starting with a reduced catalyst. A higher NO oxidation activity was observed during the heat-up phase than during the subsequent cool-down phase, indicating formation of PtO_x. The catalytic activity during the cool-down ramp was partially restored by pulses with an increased CO and C_3H_6 concentration (while still keeping lean conditions). The maximum effect of pulses was observed around the light-off temperature for CO and C_3H_6 oxidation.

A global kinetic model was developed, considering PtO_x existence and its reduction by CO and C_3H_6 pulses. The model was further validated by isothermal experiments, showing gradual decrease of NO oxidation activity and its recovery by CO and C_3H_6 at several different temperatures.

1. Introduction

The NO_x reduction efficiency in SCR and NO_x storage and reduction catalysts (NSRC), also known as lean NO_x trap (LNT), depends on NO_2/NO_x ratio in the exhaust gas. NO_2 adsorbs in a significantly greater extent than NO in the presence or absence of O_2 in LNT [1]. The NO_2/NO_x ratio of 0.5 increases the SCR catalyst activity at low temperatures thanks to the so-called fast SCR reaction [2]. NO oxidation in diesel oxidation catalyst (DOC) located in front of the deNO_x catalysts therefore significantly affects the overall function of the combined aftertreatment system. The highest conversion to NO_2 is usually reached around 250–300 °C, above this temperature, NO_2 dissociation (backward reaction) begins due to the thermodynamic equilibrium of the reaction [3].

NO oxidation activity can be influenced by several aspects. An increased O_2 concentration positively affects the NO conversion [3,4], while a high NO and/or NO_2 concentration in the gas feed results in a decrease of the NO conversion [3,5]. Three independent studies [6–8] showed a regular activity decrease during the NO oxidation caused by the presence of 5–6% water in the gas mixture over Pt/Al_2O_3. Apparent structure sensitivity of the reaction was also studied. Mulla et al. [9] and Boubnov et al. [10] reported that a higher Pt dispersion resulted in the lower NO oxidation activity. Olsson and Fridell [11] investigated the change in activity with increasing pretreatment temperature during NO oxidation and NO_2 dissociation, showing the highest activity after the pretreatment at 750 °C as the Pt catalyst became more sintered. The aging atmosphere is also an important factor. Auvray et al. [12] found out that despite a higher dispersion of a Pt/Al_2O_3 catalyst after the aging at 700 °C in O_2/Ar, the catalyst exhibited a higher NO conversion than after aging in Ar only at the same temperature. The highest conversion was achieved after the aging in SO_2/Ar and $O_2 + SO_2$/Ar, although the Pt dispersion after the pretreatment in SO_2/Ar was relatively high compared to the $O_2 + SO_2$/Ar aged sample. A similar conclusion was reported previously in [13]. XPS measurements after oxidative pretreatments [9,11] indicated the existence of platinum oxides, namely PtO and PtO_2, in general denoted PtO_x. It was

* Corresponding author.
E-mail address: petr.koci@vscht.cz (P. Kočí).
URL: http://www.vscht.cz/monolith (P. Kočí).

http://dx.doi.org/10.1016/j.apcatb.2015.08.004
0926-3373/

suggested that larger particles are more resistant toward platinum oxides formation, which can be attributed to the weaker interaction of larger particles (>7 nm) with oxygen [9].

The impact of catalyst composition on PtO_x formation was investigated by Auvray and Olsson [7] and Olsson et al. [8]. While Al_2O_3 and TiO_2 supported platinum catalysts exhibited a decrease in their activity during isothermal NO oxidation, a $Pt/V_2O_5/TiO_2$ catalyst showed a lower, but stable NO conversion [8]. Addition of Pd to a Pt/Al_2O_3 also led to a suppression of NO oxidation activity decrease [7].

The changing catalytic activity due to the platinum oxides formation was reported by several authors [6,8,11,14,15]. During isothermal NO oxidation at 200 °C [14] and 250 °C [11], and NO_2 dissociation at 350 °C [11] on Pt/Al_2O_3, significant gradual decrease in the catalyst activity was observed and a steady state was not reached even after 2 h. Inverse hysteresis of NO oxidation was reported during experiments performed as a repeated temperature ramp under a constant gas feed containing NO and O_2 [6,14]. The decrease of NO conversion during the cool-down ramp following the heat-up ramp was also attributed to PtO_x formation. At temperatures below 200 °C, the catalytic activity was partially restored due to PtO_x reduction by NO and the effect was enhanced by the absence of oxygen and cooling to a lower temperature [6,14]. The presence of water in the gas mixture negatively influences PtO_x reduction by NO at lower temperatures during NO oxidation [6]. It is also possible to reduce PtO_x during operation at high temperatures. The thermal decomposition of PtO_x starts around 350 °C [14], however, a complete regeneration can be achieved only above 650 °C [3].

Mulla et al. [9] found out that a complete PtO_x reduction can be achieved within 3 min at 160 °C with 2% CO in He or 0.5% H_2 in N_2. One hour regeneration by 200 ppm NH_3 in N_2 also restored the catalyst activity [3]. However, such conditions are impossible to achieve in practical operation of a Diesel engine. In this study, we present experimental and modeling results showing that PtO_x can be reduced by CO and C_3H_6 pulses while keeping overall lean (oxidizing) composition of exhaust gas that is natural for Diesel engines. We propose a makrokinetic model of an oxidation catalyst considering reaction rate dependence on the actual platinum oxidation state. The model includes slow oxidation of Pt by NO_2 and O_2, PtO_x thermal decomposition, PtO_x reduction by NO, and PtO_x reduction by CO and C_3H_6.

2. Experimental setup

A commercial diesel oxidation catalyst containing Pt in alumina-based support was used in the experiments. The catalyst was coated on 300 cpsi ceramic monolith. At the beginning, the catalyst was conditioned in mixture of synthetic air with 10% H_2O at 700 °C for 12 h. Before each experiment, the catalyst was pretreated in a reductive atmosphere consisting of 3% H_2 in N_2 at 370 °C for 15 min. The experiments were carried out in an adiabatic laboratory reactor with synthetic exhaust gas. The gas hourly space velocity (GHSV) was 40 000 h^{-1}.

The gas feed composition is given in Table 1. Temperature ramp experiments were repeated with and without the reactivation CO

Table 1
Inlet gas compositions.

Species	Concentration
NO	250 ppm
CO	–/1000 ppm
C_3H_6	–/111 ppm
O_2	8%
CO_2	8%
H_2O	8%
N_2	Balance

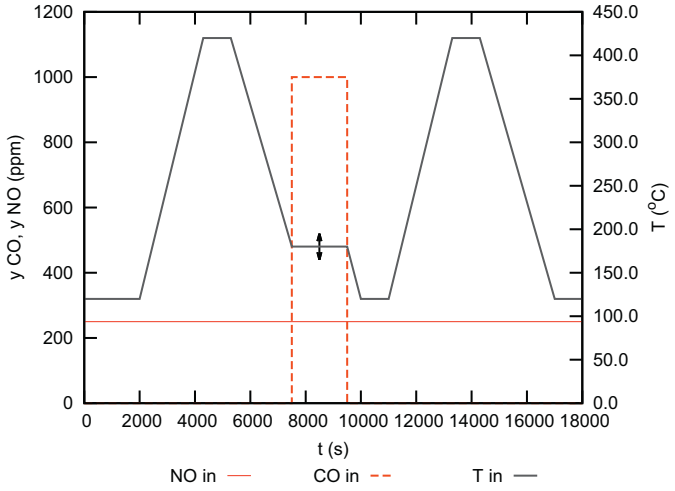

Fig. 1. Arrangement of temperature-ramp experiments with CO pulses during the reactivation period. Three different reactivation temperatures were tested: 180, 200 or 220 °C.

or C_3H_6 pulses. The experiments involved heat-up and cool-down phases to reveal the hysteresis behavior during NO oxidation. The temperature gradient was 10 K/min in the range from 120 to 420 °C. The experiments consisted of 4 parts – 2 heat-up and 2 cool-down phases. The temperature ramp was interrupted when CO or C_3H_6 pulses were applied (temperature was fixed during this period). After finishing the pulses, the temperature ramp continued. An example of the temperature program in the experiment with CO pulses is illustrated in Fig. 1. During the first cool-down phase of the experiments, CO or C_3H_6 was added into the gas mixture in the form of 5 s long pulses to reactivate the catalyst surface. The number of pulses was 30 and after each pulse, there was a pause of 60 s. Afterwards, the catalyst was cooled down to 120 °C in the gas mixture without reductants. For comparison, the second heat-up and cool-down run was carried out without pulses. The experiment was repeated several times, testing the application of CO or C_3H_6 pulses at 180, 200 or 220 °C.

Additional isothermal deactivation and reactivation experiments were carried out at constant temperature from 150 to 250 °C in steps of 25 °C. During the deactivation part, the decrease of the catalytic activity was observed under isothermal conditions. A reactivation part of the experiments was measured with the same composition and timing of pulses of CO or C_3H_6.

3. Mathematical model

The above-described experimental data were utilized in the evaluation of model kinetic parameters for the considered reactions. The objective was to develop a global kinetic model with the minimum number of employed reactions that are able to describe consistently the observed phenomena: inverse hysteresis, varying catalytic activity during isothermal NO oxidation, and increase in the activity after CO and C_3H_6 pulses. The proposed reaction mechanism involving platinum oxide formation and reduction is shown Table 2.

Temperature-dependent reaction rate coefficients are calculated using the Arrhenius equation:

$$k_j = k_{0,j}\exp\left(\frac{-E_{a,j}}{R^g T}\right). \quad (1)$$

Here j is index of reaction.

Table 2
Reactions considered in the mathematical model.

	Reaction	Reaction rate in catalytic washcoat (mol s^{-1} m^{-3})
1	$CO + \frac{1}{2}O_2 \longrightarrow CO_2$	$R_1 = k_1 \Psi_{Pt}^{cap} y_{CO} y_{O_2}/G_1$
2	$C_3H_6 + \frac{9}{2}O_2 \longrightarrow 3CO_2 + 3H_2O$	$R_2 = k_2 \Psi_{Pt}^{cap} y_{C_3H_6} y_{O_2}/G_1$
3	$NO + \frac{1}{2}O_2 \rightleftharpoons NO_2$	$R_3 = k_3 \Psi_{Pt}^{cap}(1 - \psi_{PtO_x})[y_{NO} y_{O_2}^{0.5} - y_{NO_2}/K_{y,2}^{eq}]/G_2$
4	$CO + NO \longrightarrow CO_2 + \frac{1}{2}N_2$	$R_4 = k_4 \Psi_{Pt}^{cap} y_{NO}^{0.5} y_{CO}/G_1/G_3$
5	$C_3H_6 + 9NO \longrightarrow 3CO_2 + 3H_2O + \frac{9}{2}N_2$	$R_5 = k_5 \Psi_{Pt}^{cap} y_{NO}^{0.5} y_{C_3H_6}/G_1/G_3$
6	$CO + NO_2 \longrightarrow CO_2 + NO$	$R_6 = k_6 \Psi_{Pt}^{cap} y_{NO_2} y_{CO}/G_4$
7	$C_3H_6 + 9NO_2 \longrightarrow 3CO_2 + 3H_2O + 9NO$	$R_7 = k_7 \Psi_{Pt}^{cap} y_{NO_2} y_{C_3H_6}/G_4$
8	$Pt + \frac{1}{2}O_2 \longrightarrow PtO_x$	$R_8 = k_8 \Psi_{Pt}^{cap}(1 - \psi_{PtO_x}) y_{O_2}^{0.5}$
9	$Pt + NO_2 \longrightarrow PtO_x + NO$	$R_9 = k_9 \Psi_{Pt}^{cap}(1 - \psi_{PtO_x}) y_{NO_2}$
10	$PtO_x + NO \longrightarrow Pt + NO_2$	$R_{10} = k_{10} \Psi_{Pt}^{cap} \psi_{PtO_x} y_{NO}/G_5$
11	$PtO_x + CO \longrightarrow Pt + CO_2$	$R_{11} = k_{11} \Psi_{Pt}^{cap} \psi_{PtO_x} y_{CO}$
12	$PtO_x + \frac{1}{9}C_3H_6 \longrightarrow Pt + \frac{1}{3}CO_2 + \frac{1}{3}H_2O$	$R_{12} = k_{12} \Psi_{Pt}^{cap} \psi_{PtO_x} y_{C_3H_6}$
13	$PtO_x \longrightarrow Pt + \frac{1}{2}O_2$	$R_{13} = k_{13} \Psi_{Pt}^{cap} \psi_{PtO_x}$

The inhibition terms G_1–G_5 and inhibition coefficients $K_{inh,l}$ are calculated as follows:

$$G_1 = (1 + K_{inh,1} y_{CO} + K_{inh,2} y_{C_3H_6})^2 (1 + K_{inh,3} y_{NO_x}^{0.7}) T \quad (2)$$

$$G_2 = (1 + K_{inh,4} y_{CO} + K_{inh,5} y_{C_3H_6})^2 (1 + K_{inh,6} y_{NO}^{0.7} + K_{inh,7} y_{NO_2}^{0.7}) T \quad (3)$$

$$G_3 = 1 + K_{inh,8} y_{O_2} \quad (4)$$

$$G_4 = (1 + K_{inh,9} y_{CO})(1 + K_{inh,10} y_{C_3H_6}) \quad (5)$$

$$G_5 = (1 + K_{inh,11} y_{NO} + K_{inh,12} y_{NO_2}) \quad (6)$$

$$K_{inh,l} = K_{inh,0,l} \exp\left(\frac{E_{inh,l}}{T}\right). \quad (7)$$

Here l is index of inhibition coefficient.

From the previous studies [6,11,14], it is known that NO oxidation (reaction 3) is strongly affected by the actual Pt sites state. The dependence on PtO_x coverage is reflected in the rate law of reaction 3 in Table 2. Here the catalytic activity decreases linearly with the increasing PtO_x coverage. Some authors take into account also a reaction between NO and O_2 on PtO_x, using second rate law with independent kinetic parameters [15]. In this study, this second reaction was eliminated and the catalytic activity of oxidized Pt sites was neglected in comparison with the reduced Pt sites. It was observed during the model development that the additional reaction for NO oxidation on PtO_x does not provide any significant improvement in the accuracy of model predictions.

Inhibition term G_1 in CO and C_3H_6 oxidation (reactions 1 and 2 in Table 2) considering the lumped effect of NO_x (NO and NO_2) on CO and C_3H_6 rate was adapted from Voltz et al. [17]. For NO oxidation, the inhibition by NO and NO_2 needs to be distinguished [15], which is reflected in the term G_2.

Similarly to NO oxidation, PtO_x reduction by NO (reaction 10 in Table 2) is also considered with inhibition by NO and NO_2. The self-inhibition by NO slows down PtO_x reduction at higher NO levels and prevents overshooting of PtO_x reduction rates particularly at intermediate-higher temperatures. The inhibition by NO_2 is effective mainly at lower temperatures and reflects a limited possibility of PtO_x reduction in the presence of NO_2.

Table 3
Kinetic parameters of the considered reactions in the mathematical model.

Reaction no.	k_0	E_a [kJ mol^{-1}]	Inhibition coeff.	$K_{inh,0}$	E [K]
1	6.0×10^{19}	80	$K_{inh,1}$	1.2×10^3	1.0×10^3
2	5.0×10^{20}	100	$K_{inh,2}$	1.5×10^2	2.0×10^3
3	3.9×10^{10}	35	$K_{inh,3}$	5.0×10^3	1.0×10^3
4	1.0×10^{12}	40	$K_{inh,4}$	1.6×10^1	3.0×10^3
5	1.5×10^{18}	80	$K_{inh,5}$	3.0×10^2	0.5×10^3
6	9.0×10^{15}	60	$K_{inh,6}$	5.5×10^{-8}	9.5×10^3
7	1.2×10^{16}	60	$K_{inh,7}$	6.4×10^3	-2.0×10^3
8	5.0×10^{-2}	20	$K_{inh,8}$	6.0×10^7	-8.0×10^3
9	5.0×10^2	20	$K_{inh,9}$	1.0×10^2	1.2×10^3
10	1.7×10^1	5	$K_{inh,10}$	6.0×10^2	3.0×10^3
11	3.2×10^{11}	90	$K_{inh,11}$	4.0×10^{13}	-10.0×10^3
12	1.4×10^{12}	90	$K_{inh,12}$	5.0×10^2	2.0×10^3
13	5.0×10^0	45			

Hauff et al. [14,15] attributes PtO_x formation only to O_2, whereas Hauptmann et al. [6] considers Pt oxidation caused only by NO_2. However, it is known that both O_2 and NO_2 can cause PtO_x formation. While O_2 dissociation on Pt is limited by a high oxygen coverage, the molecule of NO_2 is more coordinately flexible and able to chemisorb on an increasingly crowded surface (including high oxygen coverage) and to subsequently oxidize Pt [16]. Based on these observations, PtO_x formation by the reactions with both O_2 and NO_2 was considered (reactions 8 and 9 in Table 2). The available experimental data did not provide sufficient information to distinguish between the activation energies for these two reactions, therefore they were treated with the same activation energy. The mutual ratio of their preexponential factors was fixed at the value 1:10 000 in favor of NO_2. Obviously, the actual impact of O_2 and NO_2 depends also on the ratio of NO_2 and O_2 concentrations. Because the O_2 concentration was three orders of magnitude higher than that of NO_2 (see Table 1), the resulting effect of NO_2 on the PtO_x formation was approximately ten times greater than that of O_2. This is in line with the reported higher activity of NO_2 in PtO_x formation reactions [16].

The initial estimates of kinetic parameters were set within the range of activation energies reported in literature [6]. The parameters were then optimized by the simplex minimization method, using weighted least squares of differences between the measured and simulated outlet concentrations as the objective function. Standard, spatially 1D, heterogeneous model of the monolith channel with plug flow was employed to solve transport and reaction processes in the catalytic monolith. The model consists of mass balances in the flowing gas, mass balances in the pores of catalytic layer, mass balances on the catalyst surface sites, enthalpy balance of the flowing gas, and enthalpy balance of the solid phase, represented by the system of partial differential equations [18]. The resulting values of kinetic parameters are listed in Table 3.

4. Results and discussion

Fig. 2 shows comparison between the measured and simulated outlet NO_2 concentration during NO oxidation experiment consisting of repeated temperature ramps (first heating and cooling, second heating and cooling). The results show inverse hysteresis and they are consistent with the findings of Hauptmann et al. [6] and Hauff et al. [14]. At the beginning, fully reduced (regenerated) catalytic surface is considered. Progress of the first heat-up ramp shows catalytic NO oxidation with thermodynamic

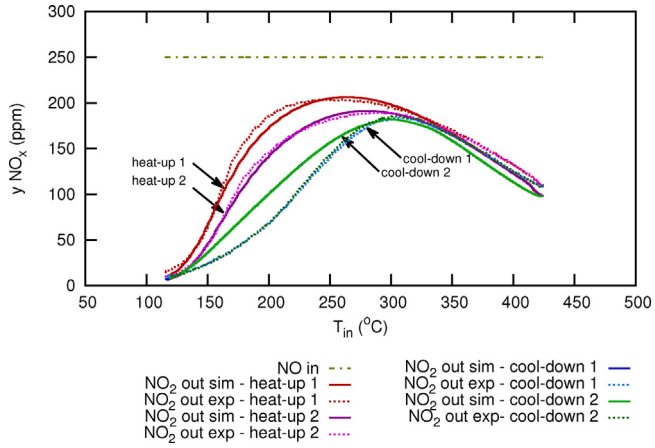

Fig. 2. Experimentally observed and simulated inverse hysteresis behavior during NO oxidation (feed: 250 ppm NO, 8% O_2, 8% CO_2 and 8% H_2O) – run 1 (after a reductive pretreatment) and run 2 (after the run 1). Each run consists of heat-up and cool-down temperature ramp.

limitation of NO_2 production at higher temperatures. The mathematical model predicts PtO_x formation gradually from the beginning as the influence of both O_2 and NO_2 is included, see Fig. 3. Even if the PtO_x coverage at higher temperatures becomes influenced by the thermal decomposition, the highest temperature reached during the ramp (420 °C) is not high enough to fully reduce all Pt sites. The decrease in the catalyst activity for NO oxidation caused by the accumulated PtO_x is obvious during the first cool-down phase (Fig. 2).

At lowest temperatures, PtO_x is partially reduced by NO (Fig. 3). After reaching 120 °C at the end of the first cool-down phase, the second heat-up ramp begins. It can be seen in Fig. 2 that the catalyst activity during the second heat-up is still lower than during the first one, indicating incomplete PtO_x reduction by NO at low temperature. Several factors contribute to the incomplete regeneration. It is known that NO can partly reduce platinum oxide at temperatures below 200 °C in spite of highly oxidizing conditions [6,14]. However, those experimental observations showed that Pt could not be fully regenerated yet at temperatures around 120–150 °C. The cool-down phase ending as low as 80 °C is needed for nearly full regeneration by NO [6]. Furthermore, such an efficient PtO_x reduction at 80 °C can be achieved only in the absence of H_2O in the feed [6] while our experiment was carried out with 8% H_2O in the feed (resembling the real exhaust gas composition). Therefore, only

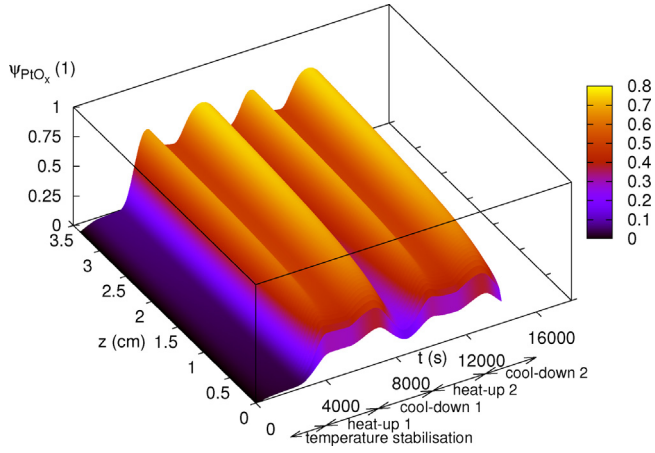

Fig. 3. Simulated PtO_x coverage profile along the monolith channel during the repeated temperature ramp (feed: 250 ppm NO, 8% O_2, 8% CO_2 and 8% H_2O).

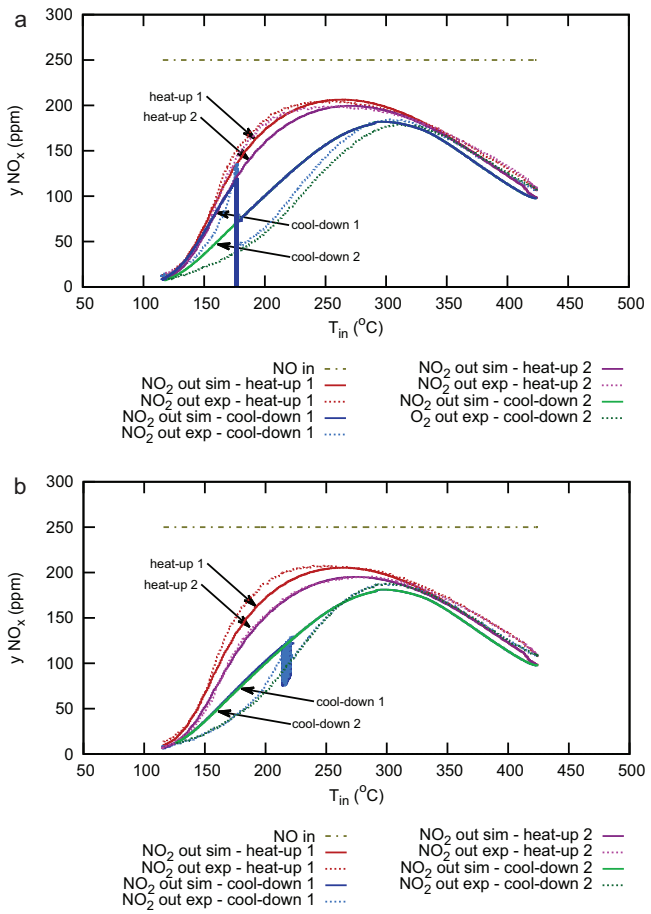

Fig. 4. NO oxidation during temperature ramp with CO pulses at (a) 180 °C, (b) 220 °C (feed: 250 ppm NO, 8% O_2, 8% CO_2 and 8% H_2O + 1000 ppm CO during pulses).

partial PtO_x reduction by NO was achieved during the cool-down phase and the model described this trend correctly.

The progress of the second cool-down ramp in Fig. 2 is the same as that of the first one. Here PtO_x thermal decomposition at higher temperatures predominates over platinum oxide formation so that the equilibrium PtO_x coverage is reached regardless of the sites state earlier during the experiment. Thus, both cool-down phases begin with the same (equilibrium) PtO_x surface fraction.

Similar experiments were then performed with a reactivation period, consisting of 30 CO or C_3H_6 pulses (each 5 s long, followed by 60 s CO/C_3H_6-free phase) applied during the first cool-down phase. The reactivation was tested in independent experiments at 180 or 200 or 220 °C.

The measured and simulated outlet NO_2 concentrations during NO oxidation experiments based on temperature ramps with CO pulses at 180 °C and 220 °C are shown in Fig. 4. The evolution corresponds to the NO oxidation experiment shown in Fig. 2 up to the part with CO pulses. In Fig. 4a, the temperature is held constant at 180 °C and CO pulses are applied in order to regenerate the catalyst activity. The influence of CO on PtO_x reduction is obvious. Fig. 5 shows the effect of CO pulses on platinum oxide surface coverage during the experiment. After the CO pulsation at 180 °C, platinum oxide is almost completely reduced and much higher outlet NO_2 concentration is observed both in simulation and experiment. The simulation results in Fig. 4a after the pulses overlap the subsequent heat-up ramp partly as the identical activity is predicted by the model for these passages. At the same time, the second heat-up ramp follows closely the progress of the first ignition ramp. Therefore for comparison, the second cool-down phase was carried out

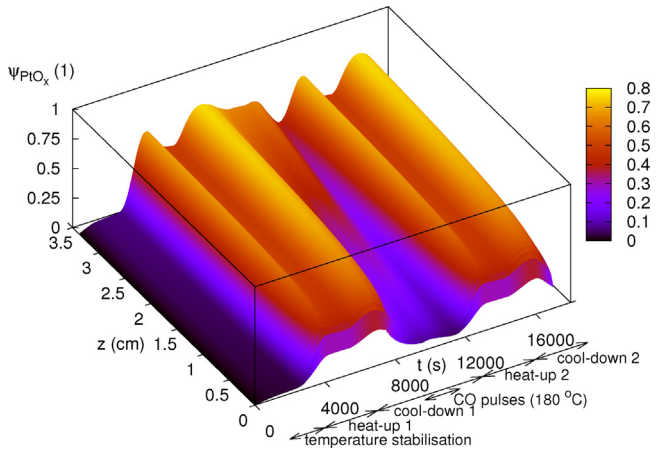

Fig. 5. Simulated PtO_x coverage profile along the monolith channel during temperature ramp with CO pulses at 180 °C (feed: 250 ppm NO, 8% O_2, 8% CO_2 and 8% H_2O + 1000 ppm CO during pulses).

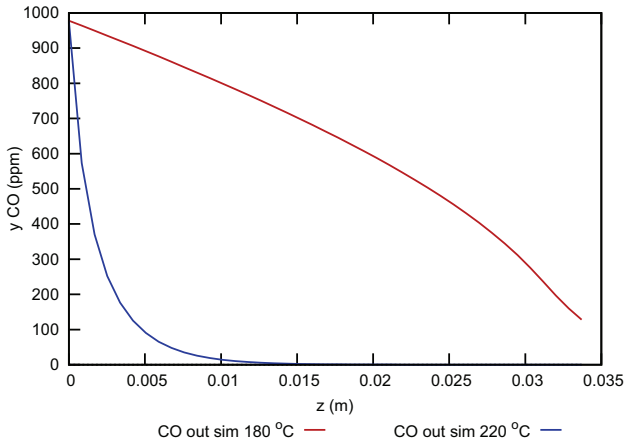

Fig. 7. Simulated CO concentration profile at 180 and 220 °C during temperature ramp with NO present in the gas mixture (feed: 250 ppm NO, 8% O_2, 8% CO_2, 8% H_2O and 1000 ppm CO).

without pulses. Here the catalyst activity remained low down to 120 °C, as no reactivation took place.

Fig. 4b shows similar experiment but the temperature of regeneration was 220 °C. It is obvious that PtO_x reduction by CO pulses is less efficient than in Fig. 4a. To understand this effect, CO oxidation rate has to be taken into account. The CO light-off temperature (at which 50% of CO oxidation conversion is reached) is ca. 175 °C in the presence of NO, cf. Fig. 6. Above this temperature, the CO oxidation rate increases rapidly and at high temperatures almost all CO is consumed in a short zone near the catalyst inlet and the rest of the catalyst remains CO-free, as shown in Fig. 7. Under such conditions only a minor fraction of PtO_x can be reduced.

To reveal the differences between the CO pulses and permanent CO feed, a heat-up and cool-down temperature ramp was measured and simulated with the gas mixture containing 1000 ppm CO during the entire experiment (Fig. 8). Both experiment and model show that the NO oxidation light-off temperature increased due to the inhibition by CO (see rate law R_3 in Table 2 and Eq. (3)), in accordance with the previously published results [6,14]. This clearly demonstrates that the constant presence of CO does not increase the NO oxidation rate. When comparing the PtO_x profiles in the permanent presence of CO (Fig. 9) and in the absence of CO (Fig. 3), it can be seen that the PtO_x coverage in the front part of the reactor is significantly lower when CO is present. However, the effect of more reduced Pt sites is counterbalanced by the inhibition of NO oxidation caused by CO. In contrast to that, the periodic

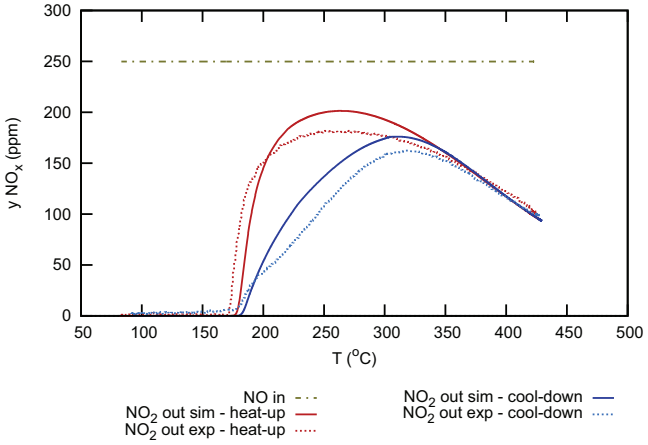

Fig. 8. NO oxidation during temperature ramp with CO (feed: 250 ppm NO, 8% O_2, 8% CO_2, 8% H_2O and 1000 ppm CO).

operation strategy with a short pulse of higher CO concentration (enabling PtO_x reduction) followed by a longer CO-free phase (minimizing the inhibition of NO oxidation) can result in a higher overall NO oxidation rate.

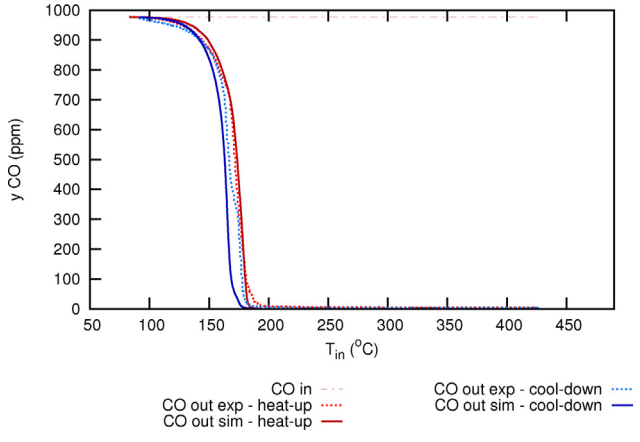

Fig. 6. CO oxidation during temperature ramp with NO present in the gas mixture (feed: 250 ppm NO, 8% O_2, 8% CO_2, 8% H_2O and 1000 ppm CO).

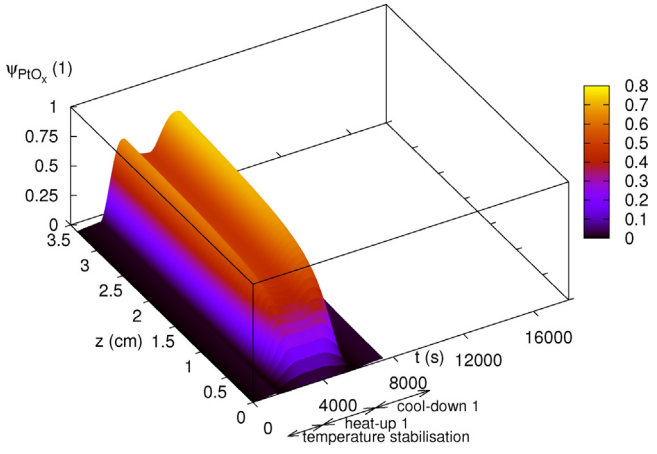

Fig. 9. Simulated PtO_x coverage profile along the monolith channel during temperature ramp with the constant CO concentration (feed: 250 ppm NO, 8% O_2, 8% CO_2, 8% H_2O and 1000 ppm CO).

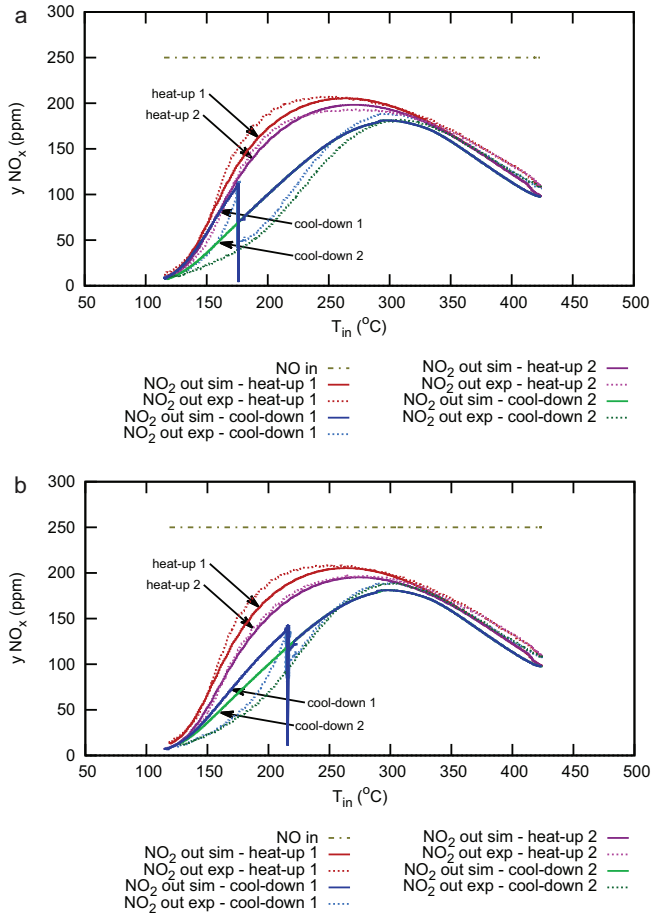

Fig. 10. NO oxidation during temperature ramp with C_3H_6 pulses at (a) 180 °C, (b) 220 °C (feed: 250 ppm NO, 8% O_2, 8 % CO_2 and 8% H_2O + 111 ppm C_3H_6 during pulses).

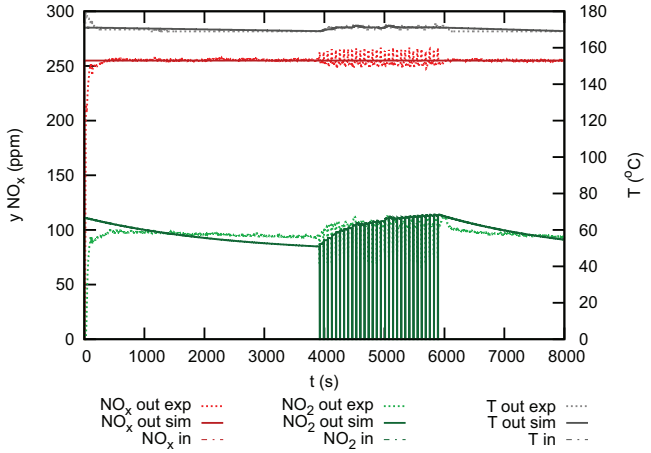

Fig. 11. Temporal progress of deactivation and reactivation during isothermal experiment at 175 °C with $\psi^{init}_{PtO_x}$ = 0.3 (feed: 250 ppm NO, 8% O_2, 8% CO_2 and 8% H_2O + 1000 ppm CO during pulses).

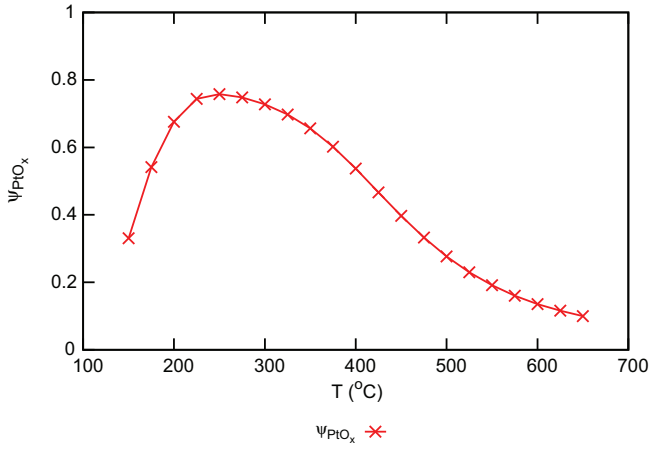

Fig. 12. Simulated steady-state PtO_x coverage (spatially averaged along the monolith channel) depending on temperature (feed: 250 ppm NO, 8% O_2, 8% CO_2 and 8% H_2O).

The reactivation by C_3H_6 pulses at 180 °C is efficient similarly to the case of CO, see Fig. 10a. Fig. 10b shows that close to the C_3H_6 light-off temperature, the PtO_x reduction by C_3H_6 pulses partially looses its impact. It can be concluded that this behaviour is similar to that of CO (cf. Fig. 4). The simulations of NO oxidation during temperature ramps have proved that the proposed mathematical model with the reactions involving platinum oxide is sufficient for prediction of the NO_2 hysteresis loop with reversible deactivation and reactivation by several mechanisms (temperature, NO, and pulses of CO or C_3H_6).

It is known that the steady state of platinum oxidation is reached not until after several hours [14]. Long isothermal experiments and simulations were performed to investigate this phenomenon further. The isothermal experiments consisted of deactivation part ($NO + O_2$ in the feed), reactivation part (with added CO or C_3H_6 pulses) and another deactivation part (at the same conditions as the first one). Fig. 11 shows the results obtained at 175 °C, which is the temperature near CO light-off in the presence of NO. At this temperature, the deactivation of Pt is relatively slow. The NO_2 concentration is low yet to cause a rapid decrease in the catalyst activity. O_2 present in excess oxidizes Pt slowly at low temperatures and the PtO_x formation gets faster only with increasing temperature [14]. Hence, even at 175 °C the PtO_x reduction by NO partly compensates the deactivation. Unfortunately, the catalyst was not perfectly reduced at the beginning of this experiment (the estimated initial PtO_x coverage was 0.3). Nevertheless, the gradual decrease of NO oxidation activity can be seen during the deactivation period in Fig. 11. The subsequent reactivation by CO pulses is very effective and noticeably increases the outlet NO_2 concentration between the pulses. The catalytic activity remains clearly higher after the pulsation period and decreases only slowly in the second deactivation period. This is in agreement with the temperature ramp experiments (Fig. 4). Similar results were obtained also during isothermal experiments with C_3H_6 pulses.

It was reported, that steady state during PtO_x formation can be reached after several hours [14,11], i.e., longer than was the duration of our experiments. Nevertheless, simulations approaching steady state were performed to verify whether the predictions of the mathematical model are consistent with those observations [14]. The isothermal simulations of steady operation with constant inlet gas composition without any reactivation pulses were carried out with 250 ppm NO, 8% O_2, 8% CO_2 and 8% H_2O in the inlet feed in the temperature range between 150 and 650 °C. Zero initial PtO_x coverage was considered. After 15 000 s (more than 4 h), steady state was reached in all cases. The steady-state PtO_x coverage (spatially averaged along the monolith channel) depending on temperature is shown in Fig. 12. The results are in good agreement with the previous studies [14,6] reporting a significant platinum oxide decomposition above 350 °C with almost full reduction at 650 °C. It can be also seen that the steady-state PtO_x coverage at

low temperatures is significantly limited by the PtO_x reduction by NO.

5. Conclusions

A reversible deactivation of NO oxidation activity caused by PtO_x formation was studied in a Pt/Al_2O_3 diesel oxidation catalyst. It was demonstrated that the catalyst activity can be restored by CO and C_3H_6 pulses while keeping overall lean conditions. Around the light-off temperature, the reactivation pulses have a substantial effect on the catalyst activity. The effect diminishes at higher temperatures due to rapid CO and C_3H_6 oxidation that consumes all reducing species in a short zone close to the catalyst inlet.

Based on the experimental observations, a global kinetic model was developed. The model captured all fundamental phenomena of NO oxidation during heat-up and cool-down temperature ramps that are affected by PtO_x formation: inverse hysteresis of NO oxidation, partial restoration of catalytic activity at low temperatures by $NO + PtO_x$ reaction, PtO_x decomposition at high temperatures, and the newly investigated PtO_x reduction and catalyst reactivation by CO and C_3H_6 pulses. The model was further validated by isothermal deactivation and reactivation experiments. The simulations of long isothermal operation revealed steady-state PtO_x coverages and confirmed the consistency with the existing studies of PtO_x formation. It was shown that the steady state of platinum oxidation can be reached after several hours and that the PtO_x coverage is increasingly limited by the PtO_x decomposition above 300 °C and by the PtO_x reduction by NO below 200 °C. The developed model can serve for design and optimization of control strategy maintaining the desired level of NO_2 formation in diesel oxidation catalyst, which is particularly important in combined exhaust gas after treatment systems including SCR catalysts and particulate filters.

Acknowledgement

The authors would like to thank Sebastian Miethe for ensuring the laboratory experiments.

References

[1] W.S. Epling, L.E. Campbell, A. Yezerets, N.W. Currier, J.E. Parks, Catal. Rev. 46 (2004) 163–245.
[2] C. Ciardellia, I. Nova, E. Tronconi, D. Chatterjee, T. Burkhardt, M. Weibel, Chem. Eng. Sci. 18–20 (2007) 5001–5006.
[3] J. Després, M. Elsener, M. Koebel, O. Kröcher, B. Schnyder, A. Wokaun, Appl. Catal. B: Environ. 50 (2004) 73–78.
[4] M.F. Irfan, J.H. Goo, S.D. Kim, S.C. Hong, Chemosphere 66 (2007) 54–59.
[5] S.S. Mulla, N. Chen, W.N. Delgass, W.S. Epling, F.H. Ribeiro, Catal. Lett. 100 (2005) 267–270.
[6] W. Hauptmann, M. Votsmeier, J. Gieshoff, A. Drochner, H. Vogel, Appl. Catal. B: Environ. 93 (2009) 22–29.
[7] X. Auvray, L. Olsson, Appl. Catal. B: Environ. 168 (2015) 342–352.
[8] L. Olsson, M. Abul-Milh, H. Karlsson, E. Jobson, P. Thormählen, A. Hinz, Top. Catal. B 30-31 (2004) 85–90.
[9] S.S. Mulla, N. Chen, L. Cumaranatunge, G.E. Blau, D.Y. Zemlyanov, W.N. Delgass, W.S. Epling, F.H. Ribeiro, J. Catal. 241 (2006) 389–399.
[10] A. Boubnov, S. Dahl, E. Johnson, A.P. Molina, S.B. Simonsen, F.M. Cano, S. Helveg, L.J. Lemus-Yegres, J.D. Grunwaldt, Appl. Catal. B: Environ. 126 (2012) 315–325.
[11] L. Olsson, E. Fridell, J. Catal. 210 (2002) 340–353.
[12] X. Auvray, T. Pingel, E. Olsson, L. Olsson, Appl. Catal. B: Environ. 129 (2013) 517–527.
[13] E. Fridell, A. Amberntsson, L. Olsson, A.W. Grant, M. Skoglundh, Top. Catal. 30-31 (2004) 143–146.
[14] K. Hauff, U. Tuttlies, G. Eigenberger, U. Nieken, Appl. Catal. B: Environ. 123–124 (2012) 107–116.
[15] K. Hauff, H. Dubbe, U. Tuttlies, G. Eigenberger, U. Nieken, Appl. Catal. B: Environ. 129 (2013) 273–281.
[16] R.B. Getman, W.F. Schneider, A.D. Smeltz, W.N. Delgass, F.H. Ribeiro, Phys. Rev. Lett. 102 (7) (2009) 076101.
[17] S.E. Voltz, C.R. Morgan, D. Liederman, S.M. Jacob, Ind. Eng. Chem. Prod. Res. Dev. 12 (1973) 294–301.
[18] A. Güthenke, D. Chatterjee, M. Weibel, N. Waldbüßer, P. Kočí, M. Marek, M. Kubíček, Chem. Eng. Sci. 62 (2007) 5357–5363.